

Cryptanalyzing a Medical Privacy Protection Scheme based on DNA Coding and Chaos

Lei Chen, Chengqing Li

Abstract—Recently, a medical privacy protection scheme (MPPS) based on DNA encoding and chaos was proposed in [IEEE Trans. Nanobioscience, vol. 16, pp. 850–858, 2017]. This paper reports some properties of MPPS and proposes a chosen-plaintext attack on it. In addition, the other claimed superiorities are questioned from the viewpoint of modern cryptography. Both theoretical analysis and experimental results are provided to support the feasibility of the attack and other security defects. The proposed cryptanalysis will promote proper application of DND encoding in protecting multimedia data including DICOM image.

Index Terms—cryptanalysis, chaotic cryptography, DNA encoding, image security, privacy protection.

I. INTRODUCTION

DNA (Deoxyribonucleic acid) encoding is widely used in medical image encryption and privacy protection in the past two decades [1], [2]. The first one is proposed in 2004 [3]. Unfortunately, some encryption schemes based on DNA encoding were reported to insecure of different extents [4]–[13].

The development of transmission and sensing technologies promote remote diagnosis (telediagnosis) and remote surgery (telesurgery). The concerns on security and privacy on the medical images transmitted on public channels are becoming more and more serious. Due to the bulky size of medical image and special storage format, the traditional text encryption standards are not efficient [14]. The directly optimized way is to reduce the size of encryption object by automatically detecting the region of interest (ROI) and leaving the region of non-interest (RONI) as plain-form. As the equivalent counterpart of cryptography, the object of cryptanalysis is to obtain the information on secret-key and/or plaintext under a given attacking scenario [15]–[18].

The randomness of the pseudo-random number sequences generated by iterating a chaotic map in digital computer may be very weaker than that of the counterpart obtained in infinite domain [19]. As reviewed in [20], various methods were proposed to counteract the dynamics degradation of digital chaotic maps: selecting state and control parameters; increasing the arithmetic precision; perturbing states; perturbing the

control parameters; switching among multiple chaotic maps; cascading multiple chaotic maps [21], [22]. The review on chaotic cryptology can be found in [23]–[25].

In [26], a medical privacy protection scheme (MPPS) based on DNA and chaos was proposed. The images stored as DICOM (Digital Imaging and Communications in Medicine) standard are encrypted with DNA encoding and PRNs generated by iterating two Coupled Chaotic Systems (CCS).

This paper focuses on security analysis of MPPS. Some properties on its essential structure are found and proved, which is then used to support an efficient chosen-plaintext attack. The metrics on validating security performance of MPPS are convincingly questioned.

The rest of the paper is structured as follows. Section II concisely present the medical privacy protection scheme under study. Detailed cryptanalyses are given in Sec. III with experimental results. The last section concludes the paper.

II. THE CONCISE DESCRIPTION OF MPPS

As specified in [26, Sec. III], MPPS can protect DICOM image data with two modes: partial and full encryption. If the former is adopted, only the significant areas for diagnosis are encrypted to considerably reduce the size of the encryption object. Except the difference on selected portions of the plain-image, MPPS works exactly the same under the two modes. Without loss of generality, the encryption object of MPPS is assumed to be a RGB color image $\mathbf{I} = \{\mathbf{I}_r, \mathbf{I}_g, \mathbf{I}_b\}$ of size $M \times N$ for either mode, which can be represented with three two-dimensional 8-bit integer matrixes: $\mathbf{I}_r = \{I_r(i, j)\}_{i=1, j=1}^{M, N}$, $\mathbf{I}_g = \{I_g(i, j)\}_{i=1, j=1}^{M, N}$ and $\mathbf{I}_b = \{I_b(i, j)\}_{i=1, j=1}^{M, N}$. Accordingly, $\mathbf{I}' = \{\mathbf{I}'_r, \mathbf{I}'_g, \mathbf{I}'_b\}$ is the cipher-image, where $\mathbf{I}'_r = \{I'_r(i, j)\}_{i=1, j=1}^{M, N}$, $\mathbf{I}'_g = \{I'_g(i, j)\}_{i=1, j=1}^{M, N}$ and $\mathbf{I}'_b = \{I'_b(i, j)\}_{i=1, j=1}^{M, N}$. Then, the basic parts of MPPS can be described as follows¹.

- The secret key is composed of six sets of initial value and control parameter $\{(Y_m(0), \mu_m)\}_{m=1}^6 = \{K_m\}_{m=1}^6$. The sub-keys K_1 and K_3 are the initial values and control parameters of Coupled Logistic-Sine (CLS) map

$$y = f(x) + \frac{1}{4} \cdot (4 - \mu) \cdot \sin(\pi x) \bmod 1, \quad (1)$$

where

$$f(x) = \mu \cdot x \cdot (1 - x) \quad (2)$$

¹To make the description more concise and complete, some details and symbols in [26] are modified under the precondition its security performance is kept unchanged.

This work was supported by the National Natural Science Foundation of China (no. 61772447).

L. Chen is with Research Institute of Information Technology (RIIT), Tsinghua University, Beijing 100084, China.

C. Li is with College of Computer Science and Electronic Engineering, Hunan University, Changsha 410082, Hunan, China (DrChengqingLi@gmail.com).

is the Logistic map. The other sub-keys, K_2 , K_4 , K_5 and K_6 , are sets of the initial values and control parameters of Coupled Logistic-Tent (CLT) map

$$y = \begin{cases} f(x) + \frac{1}{2}(4 - \mu) \cdot x \bmod 1 & \text{if } x < 0.5; \\ f(x) + \frac{1}{2}(4 - \mu) \cdot (1 - x) \bmod 1 & \text{if } x \geq 0.5, \end{cases} \quad (3)$$

where $x \in [0, 1]$, and $\mu \in [0, 4]$.

• *Initialization:*

1) *Generating index sequence:* iterate CLS map (1) t_1 times from the initial condition $Y_1(0)$ with control parameter μ_1 to avoid the transient effect; iterate it $3 \cdot M \cdot N$ more times to obtain a chaotic state sequence $\mathbf{X}_1 = \{X_1(i)\}_{i=1}^{3MN}$; sort \mathbf{X}_1 in an ascending order to generate an index sequence $\mathbf{S}_1 = \{S_1(i)\}_{i=1}^{3MN}$ satisfying that $\mathbf{X}_1(S_1(i))$ is the i -th largest element of \mathbf{X}_1 .

2) *Determining DNA coding rules:* iterate the CLT map (3) with control parameter μ_2 from the initial condition $Y_2(0)$ $t_2 = 100$ times to avoid the transient effect; iterate it six more times to obtain a chaotic sequence $\mathbf{X}_2 = \{X_2(i)\}_{i=1}^6$ and quantize it to get six random numbers $\{S_2(i)\}_{i=1}^6$ via

$$S_2(i) = \lfloor X_2(i) \times 10^{14} \rfloor \bmod 8, \quad (4)$$

where $\lfloor x \rfloor$ returns the nearest integers less than or equal to x .

3) *Constructing a pseudo-random number generator:* starting from the initial condition $Y_3(0)$, iterate CLT map (3) t_3 times with control parameter μ_3 ; iterate the map $4 \cdot M \cdot N$ more times to obtain a chaotic sequence $\mathbf{X}_3 = \{X_3(i)\}_{i=1}^{4MN}$ and quantize to a binary random sequence $\mathbf{S}_3 = \{S_3(i)\}_{i=1}^{4MN}$ by

$$S_3(i) = \begin{cases} 0 & \text{if } 0 \leq X_3(i) \leq 0.5; \\ 1 & \text{if } 0.5 < X_3(i) < 1. \end{cases} \quad (5)$$

4) *Generating three keystreams S_4, S_5, S_6 :* Similar to 1), set three sub-keys K_4, K_5 and K_6 as the control parameter and initial state of CLS map (1), generate three chaotic sequences $\mathbf{X}_4 = \{X_4(i)\}_{i=1}^{MN}$, $\mathbf{X}_5 = \{X_5(i)\}_{i=1}^{MN}$ and $\mathbf{X}_6 = \{X_6(i)\}_{i=1}^{MN}$, respectively. As above, the first t_m states are discarded for generating S_m , where $m = 4, 5, 6$. Then, every element of such sequences is quantified by

$$S_m(i) = \lfloor X_m(i) \cdot 10^{14} \rfloor \bmod 256. \quad (6)$$

• *Encryption procedure:*

a) *Permutation:* the three matrixes \mathbf{I}_r , \mathbf{I}_g , and \mathbf{I}_b are “placed” vertically to obtain a large image $\mathbf{P} = [P(i, j)]_{i=1, j=1}^{3M, N}$, where the elements of $[P(i, j)]_{i=1, j=1}^{M, N}$, $[P(i, j)]_{i=2M+1, j=1}^{2M, N}$ and $[P(i, j)]_{i=2M+1, j=1}^{3M, N}$ are set by that of \mathbf{I}_r , \mathbf{I}_g , and \mathbf{I}_b pixel by pixel, respectively. Then, produce a scrambled image $\mathbf{P}^* = \{P^*(i, j)\}_{i=1, j=1}^{3M, N}$ from \mathbf{P} by the index sequence \mathbf{S}_1 : $P^*(i, j) = P(u, v)$, where

$$\begin{cases} u = \lfloor \frac{S_1((i-1) \cdot N + j)}{N} \rfloor + 1; \\ v = S_1((i-1) \cdot N + j) \bmod N + 1. \end{cases}$$

TABLE I
EIGHT DIFFERENT DNA CODING RULES

Rule number	(00) ₂	(01) ₂	(10) ₂	(11) ₂
1	A	C	G	T
2	A	G	C	T
3	T	G	C	A
4	T	C	G	A
5	C	A	T	G
6	C	T	A	G
7	G	A	T	C
8	G	T	A	C

b) *DNA Encoding:* First, assign $E_i = X_2(i)$ for $i = 1 \sim 3$. Using function

$$f(x) = (x_0, x_1, x_2, x_3) \quad (7)$$

satisfying $\sum_{i=0}^3 x_i \cdot 2^{2i} = x$ to transform every pixel of $[P^*(i, j)]_{i=1, j=1}^{M, N}$, $[P^*(i, j)]_{i=M+1, j=1}^{2M, N}$, and $[P^*(i, j)]_{i=2M+1, j=1}^{3M, N}$ into four neighboring elements of 2-bit integer matrixes of size $M \times 4N$, \mathbf{I}_r^* , \mathbf{I}_g^* , and \mathbf{I}_b^* , respectively. Finally, convert \mathbf{I}_r^* , \mathbf{I}_g^* , and \mathbf{I}_b^* into DNA symbol matrixes with the rules in the E_1 -th, E_2 -th, and E_3 -th row of Table I, respectively. Let \mathbf{R} , \mathbf{G} , and \mathbf{B} denote the corresponding results.

c) *Diffusion I with DNA complement:* Obtain matrix $\mathbf{R}^* = \{R^*(i, j)\}_{i=1, j=1}^{M, 4N}$ by

$$R^*(i, j) = \begin{cases} R(i, j) & \text{if } S_3(i) = 0; \\ g(R(i, j)) & \text{if } S_3(i) = 1, \end{cases} \quad (8)$$

where

$$g(x) = \begin{cases} T & \text{if } x = "A"; \\ C & \text{if } x = "T"; \\ G & \text{if } x = "C"; \\ A & \text{if } x = "G". \end{cases} \quad (9)$$

d) *Diffusion II:* According to DNA addition operation rules given in the Table II, calculate

$$\begin{cases} R^{**}(i, j) = R^*(i, j) \boxplus B^*(i, j) \\ R^{**}(i, j) = G^*(i, j) \boxplus R^*(i, j) \\ R^{**}(i, j) = B^*(i, j) \boxplus G^*(i, j) \end{cases} \quad (10)$$

for $i = 1 \sim M$, $j = 1 \sim 4N$.

e) *DNA Decoding:* First, assign $D_i = X_2(i+3)$ for $i = 1 \sim 3$. Then, convert DNA symbol matrixes \mathbf{R}^{**} , \mathbf{G}^{**} , and \mathbf{B}^{**} into 2-bit integer matrixes with the rule in the D_1 -th, D_2 -th, and D_3 -th rows of \mathbf{B}^{**} , respectively. Accordingly, \mathbf{B}^{**} , \mathbf{B}^{**} , and \mathbf{B}^{**} are generated. Finally, transform \mathbf{R}^{**} , \mathbf{G}^{**} , and \mathbf{B}^{**} into \mathbf{I}_r^{**} , \mathbf{I}_g^{**} , and \mathbf{I}_b^{**} , respectively. In such transforms, every four 2-bit integer elements are merged into one 8-bit integer with the inverse function of Eq. (7).

f) *Diffusion III:* Considering every 2-D matrix as a 1-D sequence by scanning it in the raster order, obtain $\mathbf{I}'_r, \mathbf{I}'_g, \mathbf{I}'_b$ by calculating

$$\begin{cases} \mathbf{I}'_r(i) = \mathbf{I}'_r(i-1) \oplus \mathbf{I}_r^{**}(i) \oplus S_4(i) \\ \mathbf{I}'_g(i) = \mathbf{I}'_g(i-1) \oplus \mathbf{I}_g^{**}(i) \oplus \mathbf{I}_b^{**}(i) \oplus S_5(i) \\ \mathbf{I}'_b(i) = \mathbf{I}'_b(i-1) \oplus \mathbf{I}_b^{**}(i) \oplus \mathbf{I}_r^{**}(i) \oplus S_6(i) \end{cases} \quad (11)$$

for $i = 1 \sim MN$, \oplus denotes the bitwise exclusive OR operation, $I'_r(0) = 0$, $I'_g(0) = 0$ and $I'_b(0) = 0$.

- *Decryption procedure:* The decryption procedure is the inverse of the above encryption procedure. The DNA subtraction rules are shown in Table III.

TABLE II
DNA ADDITION RULES

\boxplus	A	G	C	T
A	A	G	C	T
G	G	C	T	A
C	C	T	A	G
T	T	A	G	C

TABLE III
DNA SUBTRACTION RULES

\boxminus	A	G	C	T
A	A	T	C	G
G	G	A	T	C
C	C	G	A	T
T	T	C	G	A

III. CRYPTANALYSIS OF MPPS

In this section, some properties related to MPPS and DNA coding are first analyzed. Then a detailed cryptanalysis under chosen-plaintext attack is proposed. Next attack process and simulation results are given. Evaluation on other attack analysis is finally presented.

A. Some properties of MPPS

Before the cryptanalysis, some properties of MPPS and DNA encoding/decoding are analyzed and summarized.

Property 1. Given two arbitrary cipher-images, $C_u = [C_u(i)]_{i=1}^{3MN}$ and $C_v = [C_v(i)]_{i=1}^{3MN}$, their difference ΔC is independent of the keys or equivalent keys K_4 (S_4), K_5 (S_5) and K_6 (S_6), where $\Delta C = C_u \oplus C_v = [C_u(i) \oplus C_v(i)]_{i=1}^{3MN}$.

Proof: Observing Eq. (11), one has

$$\begin{cases} \Delta C_r(i) \oplus \Delta C_r(i-1) = \Delta \tilde{C}_r(i); \\ \Delta C_g(i) \oplus \Delta C_g(i-1) = \Delta \tilde{C}_g(i) \oplus \Delta \tilde{C}_b(i); \\ \Delta C_b(i) \oplus \Delta C_b(i-1) = \Delta \tilde{C}_b(i) \oplus \Delta \tilde{C}_r(i), \end{cases} \quad (12)$$

where $\Delta \varphi = \varphi_u \oplus \varphi_v$ and $\varphi \in \{C_r(i), C_g(i), C_b(i), \tilde{C}_r(i), \tilde{C}_g(i), \tilde{C}_b(i)\}$. Hence the property is proved. ■

For convenience, here we define two composite functions $F_{i,j}(x) = f_j^{-1}[f_i(x)]$ and $G_{i,j}(x) = f_j^{-1}[g[f_i(x)]]$, where $f_i(x)$, $f_j^{-1}(x)$ and $g(x)$ are the DNA coding, decoding and transformation mentioned in the previous section, where $x \in Z_4$ and $i, j \in Z_8$.

Property 2. If $x_1, x_2 \in x$ and $x_1 \oplus x_2 = (11)_2 = 3$,

$$F_{i,j}(x_1) \oplus F_{i,j}(x_2) \neq G_{i,j}(x_1) \oplus G_{i,j}(x_2). \quad (13)$$

Proof: Considering the complementary of DNA (i.e., A and T, C and G), for $i \in Z_8$, there exists

$$(f_i(x_1), f_i(x_2)) \in \{(A, T), (T, A), (C, G), (G, C)\}.$$

According to Eq. (9), one has

$$(g[f_i(x_1)], g[f_i(x_2)]) \in \{(T, C), (C, T), (G, A), (A, G)\}.$$

For $i, j \in Z_8$, if $x_1 \oplus x_2 = (11)_2 = 3$, then

$$\begin{cases} F_{i,j}(x_1) \oplus F_{i,j}(x_2) = (11)_2, \\ G_{i,j}(x_1) \oplus G_{i,j}(x_2) = (10)_2 \text{ or } (01)_2. \end{cases} \quad (14)$$

Obviously, $F_{i,j}(x_1) \oplus F_{i,j}(x_2) \neq G_{i,j}(x_1) \oplus G_{i,j}(x_2)$. ■

Property 3. The composite functions $F_{i,j}(x)$ and $G_{i,j}(x)$ are bidirectional maps defined in domain Z_4 , and they only have 8 and 16 different maps, respectively.

Proof: First, since $f_i(x)$ and $f_j^{-1}(x)$ for $i, j \in Z_8$ and $g(x)$ are fixed bidirectional maps in domain Z_4 , $F_{i,j}(x) = f_j^{-1}[f_i(x)]$ and $G_{i,j}(x) = f_j^{-1}[g[f_i(x)]]$ are also fixed bidirectional maps. Considering the constraints of Eq. (14), one can determine the number of satisfied maps of $F_{i,j}(x)$ and $G_{i,j}(x)$ is $C_2^1 C_2^1 C_2^1 = 8$ and $C_4^1 C_2^1 C_2^1 = 16$, respectively. ■

Property 4. If $i_1, i_2 \in i, j_1, j_2 \in j$, there are two different maps $F_{i_1, j_1}(x)$, $F_{i_2, j_2}(x)$ satisfying

$$F_{i_1, j_1}(x) \oplus F_{i_2, j_2}(x) = \lambda \quad (16)$$

for $x = 0, 1, 2, 3$, where $\lambda = 1, 2$ or 3 .

Proof: The above proposition is equivalent to another proposition: if $F_{i_1, j_1}(x)$ is one of maps of $F_{i,j}(x)$, then $F_{i_2, j_2}(x) = F_{i_1, j_1}(x) \oplus \lambda$ is another map. Since $F_{i_2, j_2}(x_1) \oplus F_{i_2, j_2}(x_2) = F_{i_1, j_1}(x_1) \oplus F_{i_1, j_1}(x_2)$, $x_1, x_2 \in x$, according to Property 2, $F_{i_2, j_2}(x_1)$ is another map of $F_{i,j}(x)$. ■

Property 5. If $i_1, i_2 \in i, j_1, j_2 \in j$, there are two different maps $G_{i_1, j_1}(x) \neq G_{i_2, j_2}(x)$ satisfying

$$G_{i_1, j_1}(x) \oplus G_{i_2, j_2}(x) = \lambda \quad (17)$$

for $x = 0, 1, 2, 3$, where $\lambda = 1, 2$ or 3 .

Proof: The proof is similar to that of Property 4. ■

TABLE IV
THE ORIGINAL KEYS AND THE CORRESPONDING EQUIVALENT KEYS OF MPPS.

Original keys	Corresponding equivalent keys	Related information
K_1	S_1	Permutation index sequence
K_2	E_1, E_2, E_3 and D_1, D_2, D_3	DNA coding and decoding rules
K_3	S_3	Binary sequence
K_4	S_4	Keystream of r plane
K_5	S_5	Keystream of g plane
K_6	S_6	Keystream of b plane

B. Breaking MPPS under chosen-plaintext attack

The corresponding equivalent keys and related information of the six keys of MPPS are shown in Table IV. The goal of cryptanalysis of the paper is to reveal these equivalent keys under chosen-plaintext attack.

First, we choose a group of color plain-images whose all pixel values are equal, represented as a set of images $\mathcal{P} = \{\mathbf{P}_0, \mathbf{P}_1, \dots, \mathbf{P}_{255}\}$ where $\mathbf{P}_0 = \{0, 0, 0, \dots, 0\}$, $\mathbf{P}_1 = \{1, 1, 1, \dots, 1\}$ and $\mathbf{P}_{255} = \{255, 255, 255, \dots, 255\}$. Suppose their corresponding cipher-images set is $\mathcal{C} = \{\mathbf{C}_0, \mathbf{C}_1, \dots, \mathbf{C}_{255}\}$. Obviously, these images before and after the permutation are unchanged, that is, the corresponding images satisfy $\tilde{\mathbf{P}}_0 = \mathbf{P}_0$, $\tilde{\mathbf{P}}_1 = \mathbf{P}_1$, ..., $\tilde{\mathbf{P}}_{255} = \mathbf{P}_{255}$. Hence, we only need to focus on all intermediate states from the permutation-images to the cipher-images. Recall the description of MPPS, the DNA coding and diffusion operations after the permutation are carried out in the r , g and b planes of the images respectively. To reveal the keys of these planes, a divide-and-conquer strategy is adapted in the cryptanalysis as follows.

1) *Cracking the r plane:* In this plane, we will reveal the equivalent keys E_1, D_1, S_3 and S_4 . First, choose two special images $\mathbf{P}_{\alpha 1}, \mathbf{P}_{\alpha 2}$, which satisfy $\mathbf{P}_{\alpha 1}, \mathbf{P}_{\alpha 2} \in \mathcal{P}$ and $\mathbf{P}_{\alpha 1} \boxplus \mathbf{P}_{\alpha 2} = \mathbf{P}_{255}$. Obviously, there are $(C_4^1)^4 = 256$ plain-image pairs in set \mathcal{P} that meet. As mentioned earlier, their permutation-images are unchanged, i.e., $\tilde{\mathbf{P}}_{\alpha 1} = \mathbf{P}_{\alpha 1}$ and $\tilde{\mathbf{P}}_{\alpha 2} = \mathbf{P}_{\alpha 2}$. Subsequently, in the r plane of $\tilde{\mathbf{P}}_{\alpha 1}$ and $\tilde{\mathbf{P}}_{\alpha 2}$, each of two-bit elements (denoted as $x_1 = \alpha 1 \bmod 4$ and $x_2 = \alpha 2 \bmod 4$) is DNA encoded ($f_i(x_k)$), transformed (Eqs. (8,9)) and decoded ($f_j^{-1}(x_k)$), then the output $I_{R1_s}(k)$ can be represented in two forms

$$I_{R1_s}(k) = \begin{cases} F_{i,j}(x_k), & \text{if } S_3(k) = 0 \\ G_{i,j}(x_k), & \text{if } S_3(k) = 1 \end{cases} \quad (18)$$

where $x_1, x_2 \in x_k$, $k = 1 \sim 4MN$ and $i, j \in Z_8$. From Property 2 and Eq. (14), the differential $\Delta I_{R1_s}(k)$ satisfies

$$\begin{cases} F_{i,j}(x_1) \oplus F_{i,j}(x_2) = (11)_2, & \text{if } S_3(k) = 0 \\ G_{i,j}(x_1) \oplus G_{i,j}(x_2) = (01)_2 \text{ or } (10)_2. & \text{if } S_3(k) = 1 \end{cases} \quad (19)$$

According to the above equation, if the output $\Delta I_{R1_s}(k)$ is known, then $S_3(k)$ can be uniquely determined. Fortunately, by Property 1 and Eq. (12), $\Delta I_{R1_s}(k)$ can be obtained by dividing $\Delta \tilde{C}_r(i)$ into four two-bit elements, and the differential pixel $\Delta C_r(i)$ is available from $\Delta C_r(i)$. So the binary sequence S_3 is revealed.

The next goal is to obtain E_1, D_1 and S_4 . Since the key space of E_1 and D_1 is very small, only $8 \times 8 = 64$, we design an effective exhaustive search method for the keys, as summarized in Algorithm 1. The main idea is that we reveal same S_4 for different plain-images when the exhaustive key E_1 and D_1 are correct. Also, considering $x \in Z_4$ for $F_{E_1, D_1}(x)$ and $G_{E_1, D_1}(x)$, so we choose only four special image pairs $(\mathbf{P}_0, \mathbf{C}_0), (\mathbf{P}_{85}, \mathbf{C}_{85}), (\mathbf{P}_{170}, \mathbf{C}_{170})$, and $(\mathbf{P}_{255}, \mathbf{C}_{255})$, which correspond to different plain-pixel values $(00000000)_2, (01010101)_2, (10101010)_2$ and $(11111111)_2$, respectively. Before Algorithm 1 is executed, the plain-image

C_u will be converted to an intermediate image $CC_u, u = \{0, 1, 2, 3\}$. Formula (11) first can be converted to

$$\begin{cases} C_r(i) \oplus C_r(i-1) = \tilde{C}_r(i) \oplus S_4(i); \\ C_g(i) \oplus C_g(i-1) = \tilde{C}_g(i) \oplus \tilde{C}_b(i) \oplus S_5(i); \\ C_b(i) \oplus C_b(i-1) = \tilde{C}_b(i) \oplus \tilde{C}_r(i) \oplus S_6(i). \end{cases} \quad (20)$$

Furthermore, one has

$$\begin{cases} C_{R_s}(i) \oplus C_{R_s}(i-1) = \tilde{C}_{R_s}(i) \oplus S_4(i); \\ C_{G_s}(i) \oplus C_{G_s}(i-1) \oplus C_{R_s}(i) \oplus C_{R_s}(i-1) \oplus \\ C_{B_s}(i) \oplus C_{B_s}(i-1) \\ = \tilde{C}_{G_s}(i) \oplus S_4(i) \oplus S_5(i) \oplus S_6(i); \\ C_{B_s}(i) \oplus C_{B_s}(i-1) \oplus C_{R_s}(i) \oplus C_{R_s}(i-1) \\ = \tilde{C}_{B_s}(i) \oplus S_4(i) \oplus S_6(i). \end{cases} \quad (21)$$

The above equation shows that one can obtain three sub-images from C , i.e., $\tilde{C}_r(i) \oplus S_4, \tilde{C}_g(i) \oplus S_5 \oplus S_4 \oplus S_6$ and $\tilde{C}_b(i) \oplus S_6 \oplus S_4$ without the keys. The joint of the sub-images is defined as the intermediate cipher-image CC_u .

Interestingly, the values E_1, D_1 and S_4 searched by the Algorithm 1 are not unique. In other words, there are four equivalent classes in the table, and each class has 16 different equivalent keys, as listed in Table V. For example, suppose MPPS encrypts the r plane with $E_1 = 0$ and $D_1 = 0$, then the remaining 15 elements of the equivalent key class II can be used to decrypt. The reasons for the results are as follows:

- $F_{i,j}(x)$ and $G_{i,j}(x)$ are two kind of transformations of the r plane. From Property 3, there are 8 and 16 satisfied maps of $F_{i,j}(x)$ and $G_{i,j}(x)$, respectively, rather than the expected $8 \times 8 = 64$. Hence, there are several maps that are equivalent for different $i, j \in Z_8$.
- S_4 also has multiple equivalent keys. $S_4^{(1)}$ and $S_4^{(2)}$ are different equivalent keys only if $F_{i_1, j_1}(x) \oplus S_4^{(1)}(k) = F_{i_2, j_2}(x) \oplus S_4^{(2)}(k)$ and $G_{i_1, j_1}(x) \oplus S_4^{(1)}(k) = G_{i_2, j_2}(x) \oplus S_4^{(2)}(k)$ for $x = 0, 1, 2, 3$, are holds, where $x \in Z_4$, $i, j, i', j' \in Z_8$ and $k = 1 \sim 4MN$. The above proposition is equivalent to Properties 4 and 5.

Note that these equivalent key sets in Table V are not finalized, because DNA encoding rule f_{E_1} is constrained by Eq. (10), and we will further filter to obtain the correct keys in the next subsection.

2) *Cracking the green and blue planes:* This subsection we will crack the g and b planes and further determine a correct set of equivalent keys for r plane.

First, in the g plane, we also apply the exhaustive search method with the same four plain-images and intermediate cipher-image, which is similar to Algorithm 1. But the exhaustive algorithm needs to consider the DNA coding rules f_{E_1} since the g plane is related to r plane. Overall, it needs to search $8 \times 8 \times 8 = 512$ times. Then we will reveal an equivalent set of $\{(E_1, E_2, D_2, S_5 \boxplus S_4 \boxplus S_6)\}$, and further filter a new equivalent key set of r plane.

Similarly, we will obtain another equivalent key set of $\{(E_2, E_3, D_3, S_6 \boxplus S_4)\}$ plane and the existing equivalent key sets of g is refined. Finally, we confirm the right sets of $\{S_6\}$ and $\{S_5\}$ ².

²This step is optional in the attack process. Sec.III-C will gives an example.

TABLE V
FOUR DIFFERENT EQUIVALENT KEY CLASSES FOR (E_1, D_1, S_4)

Equivalent key classes I	Equivalent key classes II	Equivalent key classes III	Equivalent key classes IV
$(0, 0, S_4^{(1,1)})$, $(4, 4, S_4^{(1,1)})$	$(0, 1, S_4^{(2,1)})$, $(4, 5, S_4^{(2,1)})$	$(1, 1, S_4^{(3,1)})$, $(5, 5, S_4^{(3,1)})$	$(1, 0, S_4^{(4,1)})$, $(5, 4, S_4^{(4,1)})$
$(0, 2, S_4^{(1,2)})$, $(4, 7, S_4^{(1,2)})$	$(0, 3, S_4^{(2,2)})$, $(4, 6, S_4^{(2,2)})$	$(1, 3, S_4^{(3,2)})$, $(5, 6, S_4^{(3,2)})$	$(1, 2, S_4^{(4,2)})$, $(5, 7, S_4^{(4,2)})$
$(0, 4, S_4^{(1,3)})$, $(4, 0, S_4^{(1,3)})$	$(0, 5, S_4^{(2,3)})$, $(4, 1, S_4^{(2,3)})$	$(1, 5, S_4^{(3,3)})$, $(5, 1, S_4^{(3,3)})$	$(1, 4, S_4^{(4,3)})$, $(5, 0, S_4^{(4,3)})$
$(0, 7, S_4^{(1,4)})$, $(4, 2, S_4^{(1,4)})$	$(0, 6, S_4^{(2,4)})$, $(4, 3, S_4^{(2,4)})$	$(1, 6, S_4^{(3,4)})$, $(5, 3, S_4^{(3,4)})$	$(1, 7, S_4^{(4,4)})$, $(5, 2, S_4^{(4,4)})$
$(2, 0, S_4^{(1,5)})$, $(7, 4, S_4^{(1,5)})$	$(2, 1, S_4^{(2,5)})$, $(7, 5, S_4^{(2,5)})$	$(3, 1, S_4^{(3,5)})$, $(6, 5, S_4^{(3,5)})$	$(3, 0, S_4^{(4,5)})$, $(6, 4, S_4^{(4,5)})$
$(2, 2, S_4^{(1,6)})$, $(7, 7, S_4^{(1,6)})$	$(2, 3, S_4^{(2,6)})$, $(7, 6, S_4^{(2,6)})$	$(3, 3, S_4^{(3,6)})$, $(6, 6, S_4^{(3,6)})$	$(3, 2, S_4^{(4,6)})$, $(6, 7, S_4^{(4,6)})$
$(2, 4, S_4^{(1,7)})$, $(7, 0, S_4^{(1,7)})$	$(2, 5, S_4^{(2,7)})$, $(7, 1, S_4^{(2,7)})$	$(3, 5, S_4^{(3,7)})$, $(6, 1, S_4^{(3,7)})$	$(3, 4, S_4^{(4,7)})$, $(6, 0, S_4^{(4,7)})$
$(2, 7, S_4^{(1,8)})$, $(7, 2, S_4^{(1,8)})$	$(2, 6, S_4^{(2,8)})$, $(7, 3, S_4^{(2,8)})$	$(3, 6, S_4^{(3,8)})$, $(6, 3, S_4^{(3,8)})$	$(3, 7, S_4^{(4,8)})$, $(6, 2, S_4^{(4,8)})$

¹ $S_4^{(i,j)}$ represents j^{th} different keystream S_4 in the i^{th} equivalent classes, where $i \in \{1, 2, 3, 4\}$, $j \in \{1, 2, \dots, 8\}$. Since the value of $S_4^{(i,j)}$ depends on the original key $(Y_4(0), \mu_4)$, only more general relationships between them are given here.

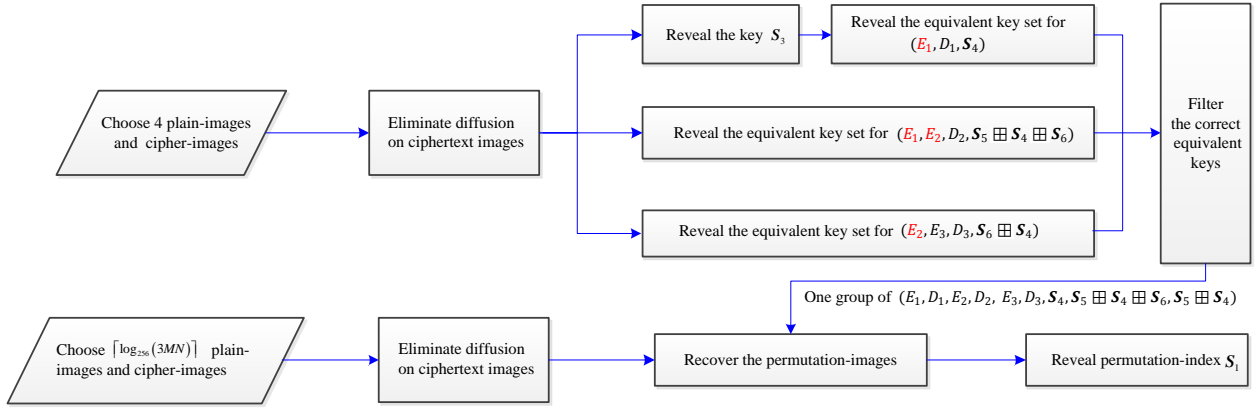


Fig. 1. Attack framework for obtaining all equivalent keys.

3) *Revealing permutation key*: Except for permutation index S_1 , now we obtain all the equivalent keys or equivalent key sets in Table IV. So, we can recover the permutation-image \tilde{P} for any cipher-image C . Then it becomes a classic cryptanalysis of permutation-only cipher problem, which has been studied in depth in [27], [28]. The general way is to use the multi-fork tree optimization method [27]. To attack MPPS, only $\lceil \log_{256}(3MN) \rceil$ plain-images are extra chosen, here $\lceil x \rceil$ returns the nearest integers more than or equal to x .

C. Attack process and simulation results

The above theoretical analysis demonstrate that MPPS is successfully broken with only $\lceil \log_{256}(3MN) \rceil + 4$ chosen plain-images. Here, a complete attack example to verify the proposed cryptanalysis method will be given.

For better presentation, assume that MPPS processes a RGB color image of size $2 \times 2 \times 3$, and the pixel value of each plane range from 0 to 255. In the following simulation, set the initial iteration of CLS or CTS map $t_0 = 500$, and six original keys of MPPS as listed in the second column of the Table VI. Accordingly, the equivalent key corresponding to the each original key is calculated by an *Initialization* procedure of MPPS.

As shown in Fig. 1, we select two group of images to obtain all the equivalent keys of MPPS. The first group includes four special plain-images and cipher-images as

$$\begin{aligned}
 P_0 &= \{0, 0, 0, 0; 0, 0, 0, 0; 0, 0, 0, 0\}, \\
 C_0 &= \{198, 60, 216, 204; 107, 69, 102, 24; 49, 72, 224, 205\}; \\
 P_{255} &= \{255, 255, 255, 255; 255, 255, 255, 255; 255, 255, 255, 255\}, \\
 C_{255} &= \{51, 158, 39, 228; 148, 69, 153, 24; 110, 234, 181, 229\}; \\
 P_{85} &= \{85, 85, 85, 85; 85, 85, 85, 85; 85, 85, 85, 85\}, \\
 C_{85} &= \{108, 60, 114, 204; 59, 20, 51, 12; 49, 72, 224, 205\}; \\
 P_{170} &= \{170, 170, 170, 170; 170, 170, 170, 170; 170, 170, 170, 170\}, \\
 C_{170} &= \{153, 158, 141, 228; 145, 20, 153, 12; 110, 234, 181, 229\}.
 \end{aligned}$$

From Eq. (20,21), the diffusion between pixels can be eliminated and a intermediate image CC_u , $u \in \{0, 255, 85, 170\}$ can be created:

$$\begin{aligned}
 CC_0 &= \{198, 250, 228, 20; 156, 173, 111, 71; 247, 131, 76, 57\}; \\
 CC_{255} &= \{51, 173, 185, 195; 201, 248, 58, 18; 93, 41, 230, 147\}; \\
 CC_{85} &= \{108, 80, 78, 190; 102, 6, 193, 172; 93, 41, 230, 147\}; \\
 CC_{170} &= \{153, 7, 19, 105; 102, 6, 193, 172; 247, 131, 76, 57\}.
 \end{aligned}$$

The differential pixel sequence of r plane between CC_0 and CC_{255} is $\{(11110101)_2, (01010111)_2, (01011101)_2, (11010111)_2\}$. By the inverse of Eq. (19), one can determine the value of the binary sequence

$$S_3 = \{0, 0, 1, 1, 1, 1, 0, 1, 1, 0, 1, 0, 1, 1, 0\}. \quad (22)$$

Algorithm 1: Exhaustive search procedure for the keys

Input: Special plain-images P_0, P_{85}, P_{170} and P_{255} and intermediate cipher-images CC_0, CC_{85}, CC_{170} and CC_{255} , DNA encoding and decoding rules $f_i, f_j^{-1}, i, j \in Z_8$, the revealed key S_3

Output: Keys E_1, D_1 and S_4

```

1 function  $Encrypt_{Rs}(P, S_3, i, j)$ 
2    $I_r \leftarrow$  obtain  $r$  plane of  $P$ ;
3    $I_{R1_s} \leftarrow$  DNA encode  $I_r$  with  $f_i$ ;
4    $\widehat{I}_{R1_s} \leftarrow$  DNA transform  $I_r$  via Eqs. (8, 9);
5    $\widehat{CC}_r \leftarrow$  DNA decode  $I_{R1_s}$  with  $f_j^{-1}$ 
6   return  $\widehat{CC}_r$ 
7  $CC_{0_r} \leftarrow$  obtain  $r$  plane of  $CC_0$ ;
8  $CC_{85_r} \leftarrow$  obtain  $r$  plane of  $CC_{85}$ ;
9  $CC_{170_r} \leftarrow$  obtain  $r$  plane of  $CC_{170}$ ;
10  $CC_{255_r} \leftarrow$  obtain  $r$  plane of  $CC_{255}$ ;
11 for  $i \leftarrow 0$  to 7 do
12   for  $j \leftarrow 0$  to 7 do
13      $K_0 \leftarrow Encrypt_{Rs}(P_0, S_3, i, j) \boxplus CC_{0_r}$ ;
14      $K_{85} \leftarrow Encrypt_{Rs}(P_{85}, S_3, i, j) \boxplus CC_{85_r}$ ;
15      $K_{170} \leftarrow Encrypt_{Rs}(P_{170}, S_3, i, j) \boxplus CC_{170_r}$ ;
16      $K_{255} \leftarrow Encrypt_{Rs}(P_{255}, S_3, i, j) \boxplus CC_{255_r}$ ;
17     if  $K_0 == K_{85} == K_{170} == K_{255}$  then
18        $E_1 \leftarrow i$ ;
19        $D_1 \leftarrow j$ ;
20        $S_4 \leftarrow K_0$ ;
21       Print keys  $E_1, D_1$  and  $S_4$ ;
22   end
23 end
24 end

```

TABLE VI

ORIGINAL KEYS SETUP AND CALCULATED EQUIVALENT KEYS FOR MPPS

Original keys	Calculated equivalent keys
$K_1 = (0.11, 3.91)$	$S_1 = \{9, 1, 10, 2, 11, 5, 7, 3, 12, 6, 4, 8\}$
$K_2 = (0.12, 3.92)$	$S_2 = \{5, 6, 6, 2, 8, 7\}$
$K_3 = (0.13, 3.93)$	$S_3 = \{0, 0, 1, 1, 1, 1, 1, 0, 1, 1, 0, 1, 1, 0, 1, 1, 0\}$
$K_4 = (0.14, 3.94)$	$S_4 = \{99, 172, 189, 130\}$
$K_5 = (0.15, 3.95)$	$S_5 = \{155, 45, 47, 189\}$
$K_6 = (0.16, 3.96)$	$S_6 = \{193, 122, 164, 238\}$

Then, input four pairs of images, $(P_0, CC_0), (P_{85}, CC_{85}), (P_{170}, CC_{170}), (P_{255}, CC_{255})$, into Algorithm 1 with S_3 . As a result, the matching equivalent keys E_1, D_1 (DNA encoding/decoding rule index) are successfully searched, and the corresponding keystreams \hat{S}_4 are also output. Similarly, multiple matching equivalent keys $(E_1, E_2, D_2, \hat{S}_5), (E_2, E_3, D_3, \hat{S}_6)$ of g and b plane, can be obtained by the key search method, respectively, where $\hat{S}_4 = S_4, \hat{S}_5 = S_5 \boxplus S_5 \boxplus S_6$ and $\hat{S}_6 = S_6 \boxplus S_4$. The corresponding results are shown in Table VII. Note that these searched keys need to be further filtered because some of them are wrong. For example, $E_1 = 2, 7, 1$ or 5 are the wrong keys because they don't appear in both key search results (the first and second columns).

Now we choose another group of images to obtain the permutation index S_1 , it includes $\lceil \log_{256}(3 \times 2 \times 2) \rceil = 1$

image. Such as a pair of plain-image and cipher-image:

$$P_{new} = \{0, 1, 2, 3; 4, 5, 6, 7; 8, 9, 10, 11\},$$

$$C_{new} = \{202, 48, 210, 196; 99, 72, 106, 17; 60, 76, 231, 205\}.$$

Select any group of keys from Table VII, such as $(E_1, D_1, \hat{S}_4) = (0, 1, \{201, 6, 23, 40\})$, $(E_1, E_2, D_2, \hat{S}_5) = (0, 1, 0, \{147, 81, 156, 123\})$ and $(E_2, E_3, D_3, \hat{S}_6) = (1, 1, 1, \{247, 131, 76, 57\})$. By Eq. (21) and keys $\hat{S}_4, \hat{S}_5, \hat{S}_6$, one can obtain an intermediate image

$$\tilde{C}_{new} = \{169, 95, 86, 148; 172, 93, 90, 150; 84, 80, 92, 80\}.$$

Then using DNA subtraction (the inverse of Eq. 10) and DNA decoding (the inverse of Eqs. 8 and 9), one can get a scrambled image

$$\tilde{P}_{new} = \{8, 0, 9, 1, 10, 4, 6, 2, 11, 5, 3, 7\}.$$

By comparing the positions of the same pixels between P_{new} and \tilde{P}_{new} , a permutation index sequence

$$S_1 = \{9, 1, 10, 2, 11, 5, 7, 3, 12, 6, 4, 8\} \quad (23)$$

can be obtained.

In general, by choosing five pairs of plain-images and cipher-images, we can uniquely determine the equivalent keys S_1 and S_3 , which are consistent with Table VI. In addition, we have eight different (E_1, D_1, \hat{S}_4) , eight (E_2, D_2, \hat{S}_5) and sixteen (E_3, D_3, \hat{S}_6) , so there are $8 \times 8 \times 16 = 1024$ groups of equivalent keys in total, and one of them is the same as in Table VI. Therefore, the proposed attack is effective and feasible.

D. Evaluation on other attack analysis

In [26, Sec. IV], the performance of MPPS was analyzed from eight aspects. In this subsection, we question their credibility one by one as follows.

1) *Key space:* The statement “it can be evident that the coupled chaotic map achieves amplified chaotic range in the entire region of $[0, 4]$ ” in [26] is questionable. The size of each sub-figure in [26, Fig. 1] is about 0.9 inch by 0.9 inch. Assume that the adopted dpi (dots per inch) is 200, the number of the printed dots is only about 32,400. Observing [26, Fig. 1], one can see that the distribution is not uniform.

Since symmetry in fixed-point arithmetic domain for initial value of CCS (1) and CLT (3) (namely, the initial values $Y(0)$ and $(1 - Y(0))$ will generate the same dynamic behavior), the effective key space of the MPPS is reduced by half. On the other hand, the initial values $Y(0) = 0, 0.5$ or 1.0 are the fixed points of CCS and CLT, which correspond to some weak keys of the MPPS. In addition, the key space of K_2 is estimated to be 10^{28} in [26], but its actual key space is only $8^6 = 2^{18}$ since six kinds of DNA encoding /decoding rules. Further, considering DNA encoding properties (Property 2, Property 3), it will generate a part of weak keys and equivalent keys. In general, the key space of MPPS is far overestimated.

2) *Key Sensitivity:* As analyzed in [28]–[30], there are many equivalent secret-key due to the dynamics degradation of chaotic system in a finite-precision computer.

3) *Statistical Attack:* Histogram analysis and entropy are unrelated with any security performance of an encryption scheme [29], [30].

TABLE VII
ALL POSSIBLE EQUIVALENT KEYS REVEALED ¹

(E_1, D_1, \hat{S}_4)	$(E_1, E_2, D_2, \hat{S}_5)$	$(E_2, E_3, D_3, \hat{S}_6)$
$(0, 1, \hat{S}_4^{(1)}), (4, 5, \hat{S}_4^{(1)})$	$(0, 1, 0, \hat{S}_5^{(1)}), (0, 5, 4, \hat{S}_5^{(1)}), (4, 1, 0, \hat{S}_5^{(1)}), (4, 5, 4, \hat{S}_5^{(1)})$	$(1, 1, 1, \hat{S}_6^{(1)}), (1, 5, 5, \hat{S}_6^{(1)}), (5, 1, 1, \hat{S}_6^{(1)}), (5, 5, 5, \hat{S}_6^{(1)})$
$(0, 3, \hat{S}_4^{(2)}), (4, 6, \hat{S}_4^{(2)})$	$(0, 1, 2, \hat{S}_5^{(2)}), (0, 5, 7, \hat{S}_5^{(2)}), (4, 1, 2, \hat{S}_5^{(2)}), (4, 5, 7, \hat{S}_5^{(2)})$	$(1, 1, 3, \hat{S}_6^{(2)}), (1, 5, 6, \hat{S}_6^{(2)}), (5, 1, 3, \hat{S}_6^{(2)}), (5, 5, 6, \hat{S}_6^{(2)})$
$(0, 5, \hat{S}_4^{(3)}), (4, 1, \hat{S}_4^{(3)})$	$(0, 1, 4, \hat{S}_5^{(3)}), (0, 5, 0, \hat{S}_5^{(3)}), (4, 1, 4, \hat{S}_5^{(3)}), (4, 5, 0, \hat{S}_5^{(3)})$	$(1, 1, 5, \hat{S}_6^{(3)}), (1, 5, 1, \hat{S}_6^{(3)}), (5, 1, 5, \hat{S}_6^{(3)}), (5, 5, 1, \hat{S}_6^{(3)})$
$(0, 6, \hat{S}_4^{(4)}), (4, 3, \hat{S}_4^{(4)})$	$(0, 1, 7, \hat{S}_5^{(4)}), (0, 5, 2, \hat{S}_5^{(4)}), (4, 1, 7, \hat{S}_5^{(4)}), (4, 5, 2, \hat{S}_5^{(4)})$	$(1, 1, 6, \hat{S}_6^{(4)}), (1, 5, 3, \hat{S}_6^{(4)}), (5, 1, 6, \hat{S}_6^{(4)}), (5, 5, 3, \hat{S}_6^{(4)})$
$(2, 1, \hat{S}_4^{(5)}), (7, 5, \hat{S}_4^{(5)})$	$(1, 0, 0, \hat{S}_5^{(5)}), (1, 4, 4, \hat{S}_5^{(5)}), (5, 0, 0, \hat{S}_5^{(5)}), (5, 4, 4, \hat{S}_5^{(5)})$	$(3, 3, 1, \hat{S}_6^{(5)}), (3, 6, 5, \hat{S}_6^{(5)}), (6, 3, 1, \hat{S}_6^{(5)}), (6, 6, 5, \hat{S}_6^{(5)})$
$(2, 3, \hat{S}_4^{(6)}), (7, 6, \hat{S}_4^{(6)})$	$(1, 0, 2, \hat{S}_5^{(6)}), (1, 4, 7, \hat{S}_5^{(6)}), (5, 0, 2, \hat{S}_5^{(6)}), (5, 4, 7, \hat{S}_5^{(6)})$	$(3, 3, 3, \hat{S}_6^{(6)}), (3, 6, 6, \hat{S}_6^{(6)}), (6, 3, 3, \hat{S}_6^{(6)}), (6, 6, 6, \hat{S}_6^{(6)})$
$(2, 5, \hat{S}_4^{(7)}), (7, 1, \hat{S}_4^{(7)})$	$(1, 0, 4, \hat{S}_5^{(7)}), (1, 4, 0, \hat{S}_5^{(7)}), (5, 0, 4, \hat{S}_5^{(7)}), (5, 4, 0, \hat{S}_5^{(7)})$	$(3, 3, 5, \hat{S}_6^{(7)}), (3, 6, 1, \hat{S}_6^{(7)}), (6, 3, 6, \hat{S}_6^{(7)}), (6, 6, 1, \hat{S}_6^{(7)})$
$(2, 6, \hat{S}_4^{(8)}), (7, 3, \hat{S}_4^{(8)})$	$(1, 0, 7, \hat{S}_5^{(8)}), (1, 4, 2, \hat{S}_5^{(8)}), (5, 0, 7, \hat{S}_5^{(8)}), (5, 4, 2, \hat{S}_5^{(8)})$	$(3, 3, 6, \hat{S}_6^{(8)}), (3, 6, 3, \hat{S}_6^{(8)}), (6, 3, 6, \hat{S}_6^{(8)}), (6, 6, 3, \hat{S}_6^{(8)})$

¹ The red number means that E_i appears in both columns, where $i = 1, 2$. For example, when E_1 in the first column is only 0 or 4, it also appears in the second column. While the underline indicates the correct equivalent keys selected, all of which have a red E_i . $\hat{S}_m^{(i)}$ represents i^{th} different keystream \hat{S}_m , where $i \in \{1, 2, \dots, 8\}$, $m \in \{4, 5, 6\}$. Due to space constraints, only certain relationships between them are given here.

4) *Differential Attack*: According to Property 1, the difference of cipher-image is unrelated to the keys S_4 , S_5 and S_6 , which will greatly reduce the effective key space. Therefore, MPPS is vulnerable to differential attack.

5) *Chosen-plaintext attack*: One specific relationship between plain-image and the corresponding cipher-image is almost unrelated with the capability of an encryption scheme against chosen-plaintext attack.

6) *Cropping Attack*: If the encryption process is not related with the plain-image, any encryption scheme is robust against cropping attack.

7) *Performance Comparison*: As emphasize in [25], any encryption scheme should target at a specific application scenario. Otherwise, the balancing point among usability, security and efficiency is unclear.

E. Other defects

1) *Practical consideration*: In [26, Sec. III], it is stated that “selection of a region of interest and region of non-interest is solely left to the user under the recommended physician”. In addition, MPPS “requires the user’s feed that specifies the number of rounds of operation”. So it requires professional training for the ordinary patients.

2) *Efficiency*: As analyzed in [29], conversion functions (4), (6) waste much computation on the discard bits. To generate a sequence of length six X_2 , $t_2 = 100$ states are sacrificed.

IV. CONCLUSION

This paper analyzed security and practical performances of a medical privacy protection scheme based on DNA encoding and chaos. Some of its properties were derived and used to obtain the equivalent secret key of the scheme with some chosen plain-images. Much works need to be done to bridge the gap between DNA computing and multimedia security.

REFERENCES

- [1] T. Xie, Y. Liu, and J. Tang, “Breaking a novel image fusion encryption algorithm based on dna sequence operation and hyper-chaotic system,” *Optik*, vol. 125, no. 24, pp. 7166–7169, 2014.
- [2] J. Wu, X. Liao, and B. Yang, “Image encryption using 2d henon-sine map and DNA approach,” *Signal Processing*, vol. 153, pp. 11–23, DEC 2018.
- [3] A. Gehani, T. LaBean, and J. Reif, “DNA-based cryptography,” *Lecture Notes in Computer Science*, vol. 2950, pp. 167–188, 2004.
- [4] Y. Liu, J. Tang, and T. Xie, “Cryptanalyzing a RGB image encryption algorithm based on DNA encoding and chaos map,” *Optics and Laser Technology*, vol. 60, pp. 111–115, AUG 2014.
- [5] H. Hermassi, A. Belazi, R. Rhouma, and S. M. Belghith, “Security analysis of an image encryption algorithm based on a dna addition combining with chaotic maps,” *Multimedia Tools and Applications*, vol. 72, no. 3, pp. 2211–2224, Oct 2014.
- [6] A. Belazi, H. Hermassi, R. Rhouma, and S. Belghith, “Algebraic analysis of a RGB image encryption algorithm based on DNA encoding and chaotic map,” *Nonlinear Dynamics*, vol. 76, no. 4, pp. 1989–2004, 2014.
- [7] Y. Zhang, “Cryptanalysis of a novel image fusion encryption algorithm based on dna sequence operation and hyper-chaotic system,” *Optik*, vol. 126, no. 2, pp. 223–229, 2015.
- [8] Y. Wang, P. Lei, H. Yang, and H. Cao, “Security analysis on a color image encryption based on dna encoding and chaos map,” *Computers & Electrical Engineering*, vol. 46, pp. 433–446, Aug 2015.
- [9] X. Su, W. Li, and H. Hu, “Cryptanalysis of a chaos-based image encryption scheme combining DNA coding and entropy,” *Multimedia Tools and Applications*, vol. 76, no. 12, pp. 14021–14033, Jun 2017.
- [10] A. Akhavan, A. Samsudin, and A. Akhshani, “Cryptanalysis of an image encryption algorithm based on DNA encoding,” *Optics and Laser Technology*, vol. 95, pp. 94–99, Oct 2017.
- [11] X. Wu, K. Wang, X. Wang, and H. Kan, “Lossless chaotic color image cryptosystem based on DNA encryption and entropy,” *Nonlinear Dynamics*, vol. 90, no. 2, pp. 855–875, Oct 2017.
- [12] H. Wen, S. Yu, and J. Lü, “Breaking an image encryption algorithm based on dna encoding and spatiotemporal chaos,” *Entropy*, vol. 21, no. 3, p. art. no. 246, 2019.
- [13] R. K. P. Kirtee Panwar and A. Jain, “Cryptanalysis and improvement of a color image encryption scheme based on dna sequences and multiple 1d chaotic maps,” *International Journal of Bifurcation and Chaos*, vol. 29, no. 8, p. art. no. 1950103, 2019.
- [14] U. R. Acharya, D. Acharya, P. S. Bhat, and U. Niranjan, “Compact storage of medical images with patient information,” *IEEE Transactions on Information Technology in Biomedicine*, vol. 5, no. 4, pp. 320–323, 2001.
- [15] F. Ozkaynak, A. B. Ozer, and S. Yavuz, “Security analysis of an image encryption algorithm based on chaos and DNA encoding,” in *Proceeding of the 21ST signal processing and communications applications conference*, 2013.
- [16] L. Chen and S. Wang, “Differential cryptanalysis of a medical image cryptosystem with multiple rounds,” *Computers in Biology and Medicine*, vol. 65, pp. 69–75, 2015.
- [17] C. Zhu and K. Sun, “Cryptanalyzing and improving a novel color image encryption algorithm using RT-enhanced chaotic tent maps,” *IEEE Access*, vol. 6, pp. 18 759–18 770, 2018.
- [18] J. Chen, F. Han, W. Qian, Y.-D. Yao, and Z.-I. Zhu, “Cryptanalysis and improvement in an image encryption scheme using combination of the 1d chaotic map,” *Nonlinear Dynamics*, vol. 93, no. 4, pp. 2399–2413, 2018.
- [19] C. Li, D. Lin, J. Lü, and F. Hao, “Cryptanalyzing an image encryption algorithm based on autoblocking and electrocardiography,” *IEEE MultiMedia*, vol. 25, no. 4, pp. 46–56, 2018.

- [20] C. Li, B. Feng, S. Li, J. Kurths, and G. Chen, "Dynamic analysis of digital chaotic maps via state-mapping networks," *IEEE Transactions on Circuits and Systems I: Regular Papers*, vol. 66, no. 6, pp. 2322–2335, 2019.
- [21] Z. Hua, S. Yi, and Y. Zhou, "Medical image encryption using high-speed scrambling and pixel adaptive diffusion," *Signal Processing*, vol. 144, pp. 134–144, MAR 2018.
- [22] Z. Hua, B. Zhou, and Y. Zhou, "Sine-transform-based chaotic system with FPGA implementation," *IEEE Transactions on Industrial Electronics*, vol. 65, no. 3, pp. 2557–2566, 2018.
- [23] G. Alvarez and S. Li, "Some basic cryptographic requirements for chaos-based cryptosystems," *International Journal of Bifurcation and Chaos*, vol. 16, no. 8, pp. 2129–2151, AUG 2006.
- [24] F. Özkaynak, "Brief review on application of nonlinear dynamics in image encryption," *Nonlinear Dynamics*, vol. 92, no. 2, pp. 305–313, 2018.
- [25] C. Li, Y. Zhang, and E. Y. Xie, "When an attacker meets a cipher-image in 2018: A Year in Review," *Journal of Information Security and Applications*, vol. 48, p. art. no. 102361, 2019.
- [26] D. Ravichandran, P. Praveenkumar, J. B. B. Rayappan, and R. Amirtharajan, "DNA chaos blend to secure medical privacy," *IEEE Transactions on Nanobioscience*, vol. 16, no. 8, pp. 850–858, Dec 2017.
- [27] C. Li and K.-T. Lo, "Optimal quantitative cryptanalysis of permutation-only multimedia ciphers against plaintext attacks," *Signal Processing*, vol. 91, no. 4, pp. 949–954, 2011.
- [28] C. Li, D. Lin, and J. Lü, "Cryptanalyzing an image-scrambling encryption algorithm of pixel bits," *IEEE MultiMedia*, vol. 24, no. 3, pp. 64–71, 2017.
- [29] C. Li, D. Lin, B. Feng, J. Lü, and F. Hao, "Cryptanalysis of a chaotic image encryption algorithm based on information entropy," *IEEE Access*, vol. 6, pp. 75 834–75 842, 2018.
- [30] M. Preishuber, T. Hutter, S. Katzenbeisser, and A. Uhl, "Depreciating motivation and empirical security analysis of chaos-based image and video encryption," *IEEE Transactions on Information Forensics and Security*, vol. 13, no. 9, pp. 2137–2150, 2018.